Biochemical and Biophysical Research Communications 450 (2014) 401–408

Contents lists available at ScienceDirect

Biochemical and Biophysical Research Communications

journal homepage: www.elsevier.com/locate/ybbrc

# Improvement of stability of nitrile hydratase via protein fragment swapping

Youtian Cui [a,1], Wenjing Cui [a,1], Zhongmei Liu [a], Li Zhou [a], Michihiko Kobayashi [b,*], Zhemin Zhou [a,*]

[a] Key Laboratory of Industrial Biotechnology, Ministry of Education, School of Biotechnology, Jiangnan University, Wuxi 214122, People's Republic of China
[b] Institute of Applied Biochemistry and the Graduate School of Life and Environmental Sciences, The University of Tsukuba, 1-1-1 Tennodai, Tsukuba, Ibaraki 305-8572, Japan

ARTICLE INFO

*Article history:*
Received 15 May 2014
Available online 2 June 2014

*Keywords:*
Nitrile hydratase
Fragment swapping
Enzyme stability
Molecular dynamics
Homologous recombination

ABSTRACT

Nitrile hydratase (NHase), which catalyzes the hydration of nitriles to amides, is the key enzyme for the production of amides in industries. However, the poor stability of this enzyme under the reaction conditions is a drawback of its industrial application. In this study, we aimed to improve the stability of NHase (*Pp*NHase) from *Pseudomonas putida* NRRL-18668 using a homologous protein fragment swapping strategy. One thermophilic NHase fragment from *Comamonas testosteroni* 5-MGAM-4D and two fragments from *Pseudonocardia thermophila* JCM3095 were selected to swap the corresponding fragments of *Pp*NHase. Seven chimeric NHases were designed using STAR (site targeted amino recombination) software and molecular dynamics to determine the crossover sites for fragment recombination. All constructed chimeric NHases showed 1.4- to 3.5-fold enhancement in thermostability and six of them become more tolerant to high-concentration product. Notably, one of these NHases, 3AB, exhibited a 1.4 ± 0.05-fold increase in activity compared to the wild-type *Pp*NHase. Circular dichroism spectrum analysis and homology modeling revealed that the 3AB slightly differed in secondary structure from wild-type *Pp*NHase. The 3AB constructed in this study is useful for further industrial application, and the method for designing the chimeric protein using homologous protein fragment swapping without a decrease in activity may be a strategy to improve the stability of other enzymes.



## 1. Introduction

Hydration of nitriles to their corresponding amides is an important reaction that not only occurs in nature but also in organic synthesis. There are two approaches for the hydration of nitriles: enzymatic hydration and chemical hydration by a catalyst, such as copper [1]. Nitrile hydratase (NHase, EC 4.2.1.84), which catalyzes the hydration of nitriles to corresponding amides is one of the key enzymes of nitrile metabolism in a large number of microorganisms [1,2]. The enzyme, which consists of α- and β-subunits, contains either non-heme iron [3] or non-corrinoid cobalt in the active site [4]. NHase has also been successfully adopted in the chemical industry for the production of acrylamide, nicotinamide and 5-cyanovaleramide [1].

One of the drawbacks in the application of NHase is their poor thermostability and stability under high-concentration product. In the bioconversion process, the additional refrigeration to maintain the activity adds the costs of energy and the high accumulation of the product makes the enzyme inactive irreversibly [5]. Although an improvement in the stability of NHase is needed for its industrial application, successful cases of protein engineering of NHase are rarely reported until recently [6].

Many protein engineering strategies have been developed to improve the stability of enzymes and some certain enzymes have been redesigned and extended to the large-scale production [7]. Among these strategies, engineering using homologous recombination could harness structural and evolutionary information to design highly mutated, yet still natively folded, chimeric proteins and protein libraries [8]. Many proteins have been successfully modified using random or rational recombination methods [9,10]. For the recombinant method, it is crucial to select the corresponding recombination fragments and optimal recombination sites. In contrast to random recombination, site-directed recombination via the identification of specific sites in parental sequences in which their parts can be interchanged, enhances the successful rates of functional protein generation [11]. Several tools are available to identify optimal recombination sites [11,12]. Using these tools and swapping protein segments, such as domains, fragments

* Corresponding authors. Fax: +81 29 853 4605 (Institute) (M. Kobayashi). Fax: +86 510 85197551 (Z. Zhou).
*E-mail addresses:* kobay@agbi.tsukuba.ac.jp (M. Kobayashi), zhmzhou@jiangnan.edu.cn (Z. Zhou).
[1] These authors contributed equally to this work.

http://dx.doi.org/10.1016/j.bbrc.2014.05.127
0006-291X/

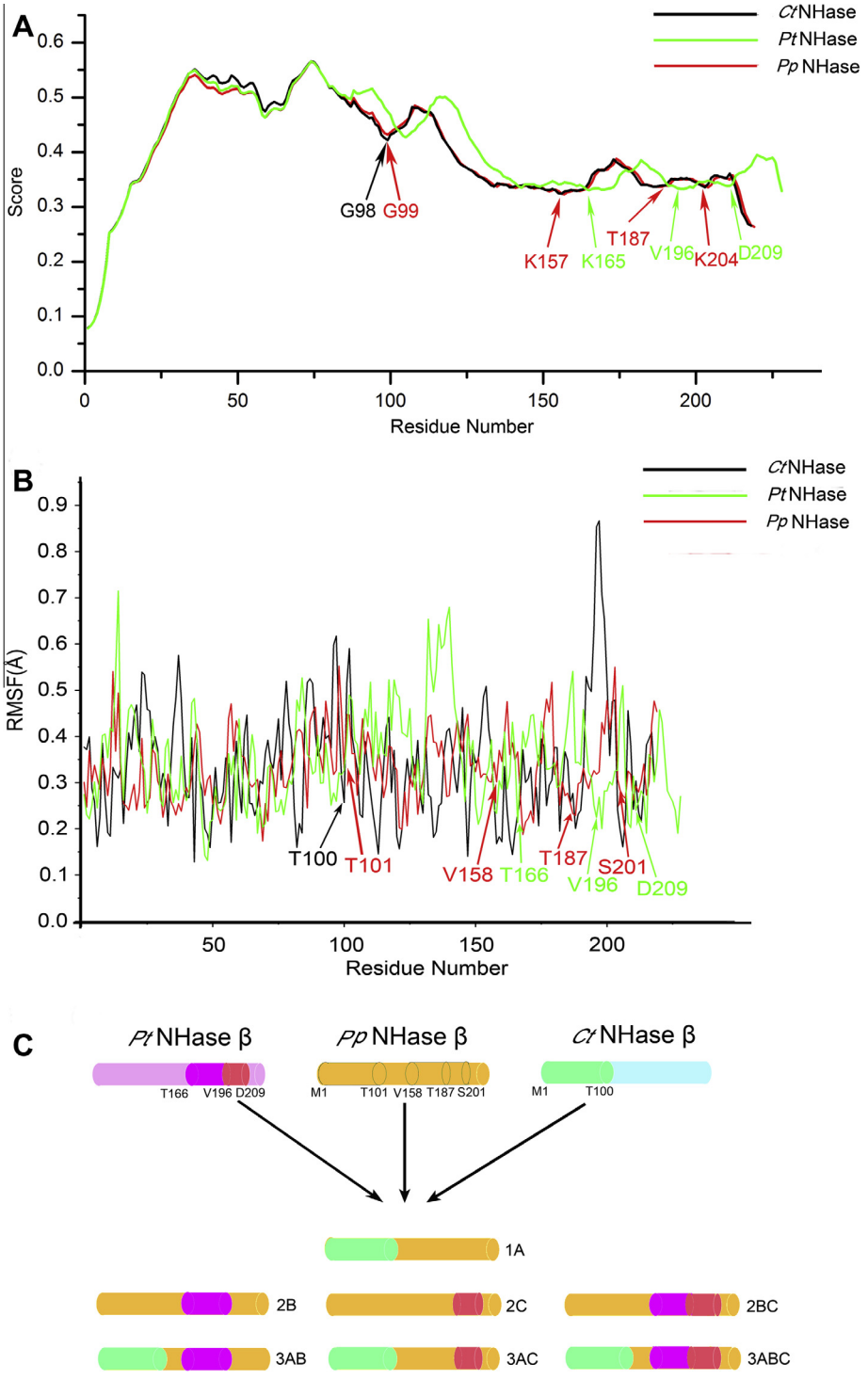


**Fig. 1.** STAR score profile, RMSF values for *Pp*NHase, *Ct*NHase and *Pt*NHase and schematic of chimeric NHases construction. (A) STAR score curves for NHases. The troughs with lower scores indicate the most potential recombination crossover sites without disturbing the structural stability. (B) RMSF obtained from 5-ns trajectories of *Pp*NHase, *Ct*NHase and *Pt*NHase. (C) Structural organization of chimeric NHases. The numbers indicate the parent NHases from which the fragments were selected. (1) *Ct*NHase; (2) *Pt*NHase; (3) both *Ct*NHase and *Pt*NHase. Wild-type *Pp*NHase is colored in orange. The fragments colored in red are from *Pt*NHase, and the one colored in green is from *Ct*NHase. Detailed organization of chimeric NHases are shown in Table 1. (For interpretation of the references to color in this figure legend, the reader is referred to the web version of this article.)

and termini, all of which stem from proteins with better qualities, could be utilized to relieve or eliminate the drawbacks of wild-type proteins.

In this study, NHase (*Pp*NHase) from *Pseudomonas putida* NRRL-18668 was modified to improve thermostability using homologous recombination. One thermophilic fragment from *Comamonas testosteroni* 5-MGAM-4D NHase (*Ct*NHase) and two fragments from *Pseudonocardia thermophila* JCM3095 NHase (*Pt*NHase) were selected to swap the corresponding fragments of *Pp*NHase, resulting in seven chimeric NHases. Although *Pp*NHase possess relatively poor stability *Ct*NHase and *Pt*NHase, it is notably that this enzyme has the higher activity, broad substrate specificity, demonstrated stereoselective, and regioselective capabilities [13,14]. The seven chimeric NHases exhibited higher thermostability than that of

the wild-type *Pp*NHase. In addition, the highest stable one termed 3AB exhibited 1.4 ± 0.05-fold in activity in comparison to the wild-type *Pp*NHase, which would be more suitable for the further industrial application of NHase.

## 2. Material and methods

### 2.1. DNA Construction

These plasmids carried the NHase genes from *C. testosteroni* 5-MGAM-4D (AY743666) and NHase from *P. thermophila* were synthesized by Shanghai Gene Core Biotechnologies Co., Ltd. (Shanghai, China). All chimeric NHases were constructed by performing two steps. The first step was to clone the swapping fragments. Each gene fragment of *Ct*NHase or *Pt*NHase was cloned by primers using Taq polymerase. All primers used in this study are listed in Table S1. Next, the purified PCR products were obtained as PCR primers to substitute the parent gene in *Pp*NHase with PrimeSTAR® HS DNA Polymerase (Takara Biotechnology (Dalian) Co., Ltd.) using a whole plasmid PCR protocol [15]. All products were transformed into *Escherichia coli* JM109.

### 2.2. Expression and purification of enzymes

*E. coli* BL21 (DE3) containing recombinant plasmids were grown at 37 °C using TB medium containing $CoCl_2$ $6H_2O$ (0.05 g/L) and kanamycin (50 mg/mL). After the $A_{600}$ reached 0.8, Isopropyl β-D-thiogalactopyranoside (IPTG) was added to a final concentration of 0.4 mM. Next, the cells were incubated at 24 °C for 16 h. All purification steps were performed at 0–4 °C using the ÄKTA Avant purification system (GE Healthcare UK Ltd.). Potassium phosphate buffer (KPB, 10 mM, pH 7.4) containing 0.5 mM dithiothreitol (DTT) was used in all purification steps. The cell extract was prepared by ultrasonics. After centrifugation for 20 min at 18,000×*g*, NHase was partially purified using ammonium sulfate fractionation (40–75%). Dialysis was followed by KPB; the dialyzed solution was applied to a Hitrap Q HP (GE Healthcare). The proteins on the column were eluted with elution buffer (a linear gradient from 0 to 0.5 M KCl in KPB). Next, the fraction was applied to Superdex 200 10/300 GL(GE Healthcare). Each step in the purification was analyzed using SDS–PAGE.

### 2.3. Enzymatic assay

The enzymatic activity for NHase was assayed in a reaction mixture (0.5 ml) containing 10 mM KPB (pH 7.5), 20 mM 3-cyanopyridine, and 5 ul of the enzyme containing the activation buffer. The reaction was performed at 20 °C for 10 min and was stopped with the addition of 0.5 ml of acetonitrile. The amount of nicotinamide formed in the reaction mixture was determined as previously described [16]. One unit of NHase activity was defined as the amount of enzyme that catalyzed the release of 1 μmol of nicotinamide per min at 20 °C. The kinetics characterization of 3AB and wild-type *Pp*NHase were assayed by changing the 3-cyanopyridine concentration ranging from 5 mM to 200 mM. Then all samples were examined and the results were calculated by Michaelis–Menten equation model.

### 2.4. Determination of the thermostability of NHases

All of the NHases with a concentration of 0.3 mg/ml were prepared in 10 mM KPB (pH 7.5). All of the samples were incubated at 50 °C and were removed at intervals of 10 min and then kept on ice. Next, the samples were assayed. The activities of these enzymes prior to heating were defined as 100%. Half-lives ($\tau 1/2$) were defined as the time during which the activities were decreased to a half.

### 2.5. Tolerance assessment to high concentration amides

To assay the different nicotinamide-tolerance of wild-type *Pp*NHase and 3AB, we slightly revised the assay method proposed by the former work [6]. We prepared cells in 0.5 M nicotinamide for 20 min. Next, 10 μl of the samples were obtained for enzymatic assay. One unit of NHase activity was defined as the amount of enzyme that catalyzed the reduction of 1 μmol of 3-cyanopyridine per min at 20 °C. The activity prior to the addition of a high concentration amide was defined as 100%.

### 2.6. Determination of the pH range of NHases

The range of pH for enzyme activity was determined by performing the assay in Britton-Robinson buffers (10 mM, pH from 5.0 to 11.0).

### 2.7. Computational design methods

Sequence alignments were performed using BLAST to identify sequence homologues. The 3D-structural model of *Ct*NHase (NHase-CT) and 3AB was generated using Modeller software based on the 3D-structure of NHase from *P. putida* NRRL-18668 (3QXE) and *P. thermophila* (1UGQ).

Two computational methods were used to determine the swapped NHase fragments and crossover sites that define these fragments. First, the STAR (site targeted amino recombination) program was used to predict the recombination positions. The amino acid sequences of NHases were examined. Next, 5-ns molecular dynamics (MD) was performed to estimate the flexibility of the backbone to accurately define the fragment swapped crossover sites. The crystal structures used in the MD simulation were 1UGQ from *P. thermophila* JCM3095 and 3QXE from *P. putida* NRRL-18668 and NHase-CT. MD was performed with NAMD 2.7 [17] and the CHARMM27 force field [18] at 300 K. The SHAKE algorithm was set on all bonds, and particle mesh Ewald was employed to compute the electrostatic interactions in the periodic boundary. After energy minimization by 1000 conjugate gradient steps, heating and 1 ns equilibration, the production phase 5 ns was performed with a step time of 2 fs.

### 2.8. Circular dichroism measurement and thermal denaturation experiments

Circular dichroism (CD) spectra were measured on the MOS-450/AF-CD-STP-A instrument at a protein concentration of 0.2 mg/ml in 1 0 mM KPB buffer. Wavelength scans were run from 195 to 250 nm to detect the second structure of the protein. Temperature melts were run with 0.05–0.2 mg/ml protein at 220 nm signal from 10 °C to 70 °C which was controlled using a Peltier device.

## 3. Results

### 3.1. Selection of fragments and crossover sites for swapping

We swapped the less thermo-sensitive regions with fragments with thermophilic features from other NHases. For the two subunits of *Pp*NHase, the α-subunit containing cobalt ion may be achieved through processes of self-subunit swapping [19,20]. To avoid the disadvantageous effect on the maturation process of *Pp*NHase, the β-subunit was selected as the engineered template.

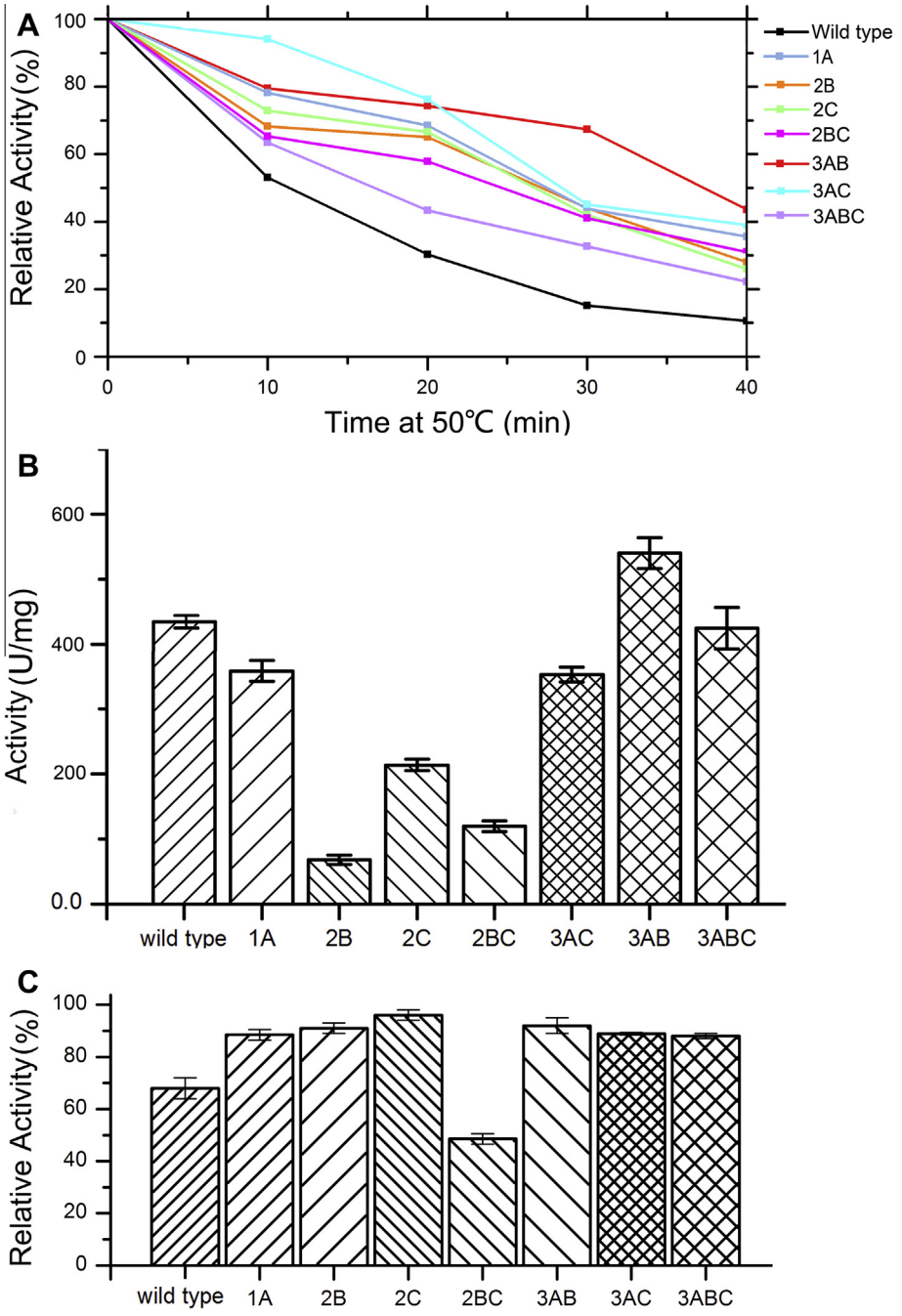


**Fig. 2.** Stabilities and activities of wild-type *Pp*NHase and chimeric NHases. (A) Comparison of the thermostability of all engineered NHases. All NHases were incubated at 50 °C, and their activities were measured over time. (B) Comparison of the activity of all engineered NHases. The values represent the means for at least triplicate independent experiments. (C) Comparison of nicotinamide-tolerance of NHases in the in-cell forms. Residual activities were assayed after immersion in 0.5 M nicotinamide for 20 min.

The N-terminus of the β-subunit in *Ct*NHase could be qualified because although *Ct*NHase shows a high homology with *Pp*NHase (beyond 80%), *Ct*NHase exhibits thermostable features, and the amino acid sequences in the N-terminus of β-subunit were relatively different [21]. In addition, the C-terminus of *Pt*NHase from *P. thermophila* was another qualified fragment because it exhibits less thermo-sensitivity as previously reported [22].

Next, we performed a two-procedure selection for recombination crossover sites. The first procedure examined the potential structural disruption caused by recombination using STAR. Lower scores in this STAR-profile represent regions where the protein structures have a lower contact density and are thus less likely to cause the overall structure destroyed and activity lost by recombination. Thus, a suitable recombination site was one with a low score [12]. According to the results of the STAR analysis in Fig. 1A, one fragment (M1 to G98 from *Ct*NHase) was selected as a substitute for the fragment M1–M99 from *Pp*NHase, and two fragments from *Pt*NHase (K165-V196 and K165-D209) were selected as substitutes for two fragments (K157-T187 and T187-K204) of *Pp*NHase, respectively. In light of the STAR analysis failing to take into account the 3D structure, which potentially affected the accuracy of the prediction of the crossover sites, molecular dynamics simulation (MD) analysis was performed to precisely define the crossover sites. The RMSF (mean square fluctuation)

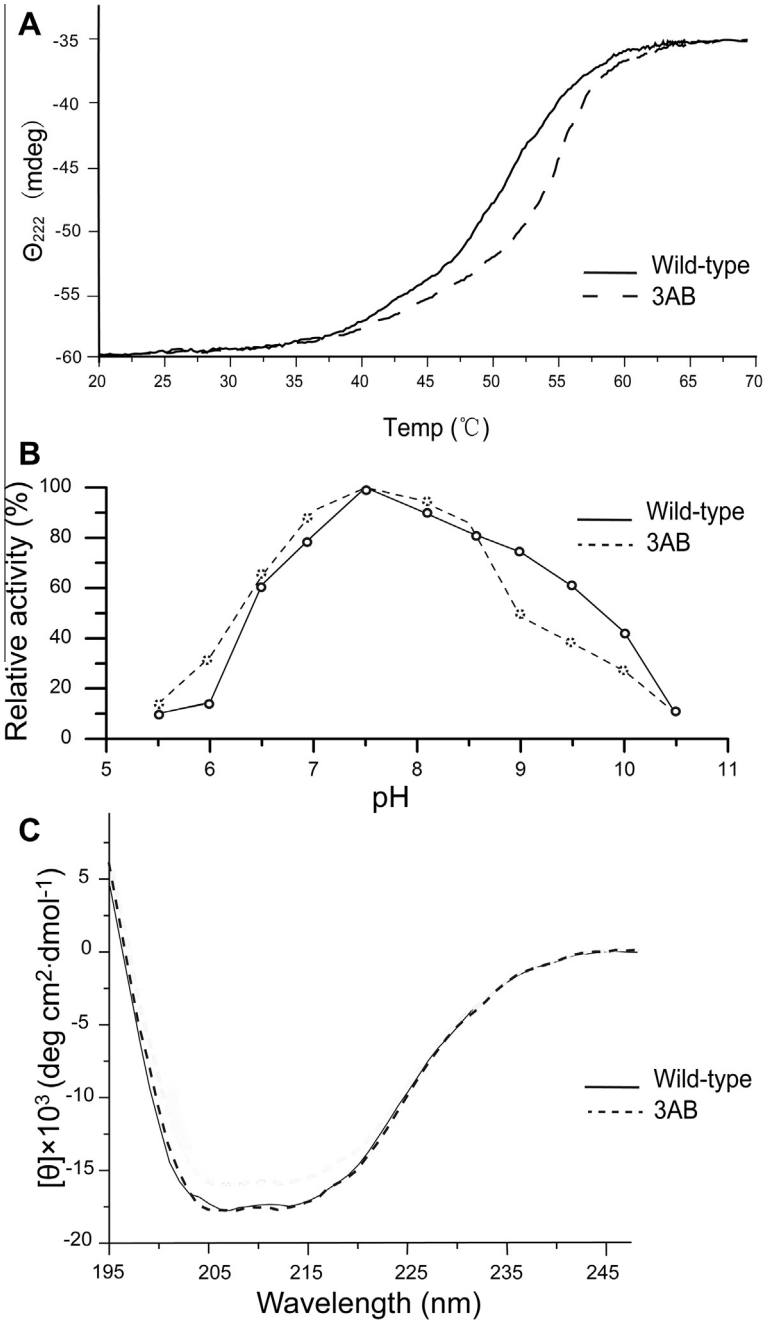


**Fig. 3.** Comparison of catalytic and structural characteristics between wild-type *Pp*NHase and 3AB. (A). Thermal denaturation experiments of NHases. Temperature-induced unfolding profile of wild-type *Pp*NHase and 3AB derived from data monitored by changes in ellipticity at 222 nm (B) The pH range profiles of 3AB and wild-type *Pp*NHase (C) CD spectrum curves of wild-type *Pp*NHase and 3AB. The data monitored in the far UV region (195–250 nm) are shown.

values, which exhibit the rigidity of each residue important for *Ct*NHases, *Pt*NHases and *Pp*NHases stabilization, are shown in Fig. 1B. According to the principle for selecting crossover sites reported by Voigt et al. [11], T166, V196, and D209 from *Pt*NHase; T100 from *Ct*NHase; and T101, V158, T187 and S201 from *Pp*NHase were selected as crossover sites due to their relatively rigid sites and around the recombination sites predicted by STAR.

### *3.2. Comparison of stability between the wild-type PpNHase and the chimeric NHases*

According to the crossover sites determined above, seven chimeric NHase genes were designed using protein swapping fragments (Fig. 1C). Each chimeric NHase gene was expressed in *E. coli* BL21(DE3) (Fig. S1) and then purified for further research. To determine the thermostability of wild-type *Pp*NHase and the chimeric NHases constructed above, the residual activity was measured as the incubation at 50 °C. As shown in Fig. 2A, the residual relative activity of each chimeric NHase was higher compared to the wild-type *Pp*NHase, and their $\tau_{1/2}$ was elongated, ranging from 1.4- to 3.5-fold, indicating that the thermostability of each chimeric NHase was improved compared to the wild-type *Pp*NHase. Importantly, 3AB exhibited the longest half-time; it preserved a 70% residual activity after incubation at 50 °C for 30 min, whereas wild-type *Pp*NHase only demonstrated 15% residual activity. In addition, two of the chimeric NHases (3AB and 3ABC) showed a

**Table 1**
Summary of designed NHase chimeras.

| Chimeric NHases | Gene organization | Total length (aa) |
|---|---|---|
| 1A | 1–100: Met1-Thr100 *Ct*NHase, 101–218: Ala102-Ala219 *Pp*NHase | 218 |
| 2B | 1–157: Met1-Lys157 *Pp*NHase, 158–188: Thr166-Val196 *Pt*NHase, 189–220: Val188-Ala219 *Pp*Nhase | 220 |
| 2C | 1–186: Met1-Tyr186 *Pp*NHase, 187–200: Val196-Asp209 *Pt*NHase, 201–218: Ser202-Ala219 *Pp*NHase | 218 |
| 2BC | 1–157: Met1-Lys157 *Pp*NHase, 158–201: Thr166-Asp209 *Pt*NHase, 202–219: Ser202-Ala219 *Pp*NHase | 219 |
| 3AB | 1–100: Met1-Thr100 *Ct*NHase, 101–156: Ala102-Lys157 *Pp*NHase, 157–187: Thr166-Val196 *Pt*NHase, 188–219:Val188-Ala219 *Pp*NHase | 219 |
| 3AC | 1–100: Met1-Thr100 *Ct*NHase, 101–185: Ala102-Tyr186 *Pp*NHase, 186–199: Val196-Asp209 *Pt*NHase, 200–217: Ser202-Ala219 *Pp*NHase | 217 |
| 3ABC | 1–100: Met1-Thr100 *Ct*NHase, 101–156: Ala102-Lys157 *Pp*NHase, 157–200: Thr166-Asp209 *Pt*NHase, 201–218: Ser202-Ala219 *Pp*NHase | 218 |

The number indicates the parent strain from which the fragments derive. 1 is *Ct*NHase, 2 is *Pt*NHase and 3 is both.

higher activity compared to wild-type NHase (Fig. 2B). The activities of 3AB and 3ABC were 1.4-fold (614 U/mg) and 1.1-fold (483 U/mg) of wild-type *Pp*NHase (439 U/mg), respectively. In addition, these chimeras with swapping fragments from *Ct*NHase and *Pt*NHase (3AB, 3AC, 3ABC) generally showed relatively higher activities than those only with one swapped fragments (1A, 2B, 2C).

Because NHases are known to undergo irreversible product inactivation [5], it is necessary to examine the stability of different chimeras under high concentration of product. As shown in the Fig. 2C, six of chimeric NHases maintained more than 85% residual activities while wild-type *Pp*NHase only maintained 68% residual activity. Two highest tolerant NHases were 2C and 3AB, maintaining 90% and 88% residual activities, respectively.

Taken together, we further investigated the 3AB, which had the highest activity, the most thermostability and higher tolerance toward amide.

### 3.3. Comparison of the melting temperature (Tm), pH and kinetic characteristics between wild-type PpNHase and the 3AB

To precisely investigate thermal tolerance between 3AB and wild-type *Pp*NHase, thermal denaturation experiments were performed. The thermal unfolding curve revealed the protein thermal tolerance related to the thermodynamic stability of the protein—its ability to refold after elevated temperature had dissipated [23]. As shown in Fig. 3A, the *T*m of 3AB was approximately 54 °C, which is 4 °C higher than wild-type *Pp*NHase (approximately 50 °C). This finding revealed that 3AB exhibited a much higher thermal tolerance than wild-type *Pp*NHase.

The stabilities of two enzymes in various pH were determined and compared. As shown in Fig. 3B, neither of them could tolerate excessive acidic condition (pH $\leqslant$ 5) and excessive basic condition (pH $\geqslant$ 11). They had the similar optimistic pH value, 7.5. The differences lay in their activities in acidic and basic conditions. 3AB had relatively higher activity when pH was among 5.5–7.5 whereas lower activity when pH was among 7.5–10.5. The kinetic parameters for the two enzymes were listed in Table 2. After fragment swapping, *K*m decreased by 9 times and *k*cat/*K*m increased by 7 times.

**Table 2**
Distinguishable catalytic properties of 3AB and *Pp*NHase.

| Enzymes | *K*m (mM) | *k*cat ($min^{-1}$) | *kcat*/*K*m ($min^{-1}$ $mM^{-1}$) |
|---|---|---|---|
| Wild-type *Pp*NHase | 53.0 ± 11.2 | 8.08 ± 0.72 | 0.15 |
| 3AB | 6.16 ± 1.52 | 6.72 ± 0.61 | 1.09 |

### 3.4. Structural analysis of the wild-type PpNHase and 3AB

CD spectrum analysis was performed to determine the differences in secondary structure between the two enzymes. As shown in Fig. 3C, the CD spectrum of 3AB was not dramatically different from that of wild-type *Pp*NHase. Since the fragments swapped from *Ct*NHase and *Pt*NHase were structurally similar with the corresponding fragments of *Pt*NHase (Fig. 4A), we were able to model the structure of 3AB. The results of homology modeling were accordant with CD spectrum (Fig. 4B). One loop change in N-terminal and the additional helix in C-terminal of 3AB may account for the slight structural differences in CD spectrum. In addition, MOLE 2.0 is software which can perform a rapid detection and analyze physical–chemical characterization of tunnels, pores and cavities in biomacromolecule [24]. Therefore, we further tested whether the swapped fragments affect the tunnel using MOLE 2.0 software. As shown in Fig. 4B, the tunnel of 3AB is formed by two swapped fragments and that of wild-type *Pp*NHase is formed by the corresponding two fragments, and the location of the tunnel does not change after fragments swapping, indicating that the fragments swapping does not lead large alteration to the tunnel for substrate and product spreading.

## 4. Discussion

To improve *Pp*NHase stability, the enzyme was engineered using a rational recombination method given that the less thermo-sensitive fragments have been reported. For a recombination method, fragment swapping has been found to be a potential method for protein rational design to enhance the stability of enzymes. To obtain correctly folded and soluble chimeric enzymes with a high stability, proper fragments and appropriate crossover sites should be identified. Thus, which residues are chosen to be the crossover sites is a crucial procedure to construct functional enzymes. Recently, several computer-aided technologies used to predict suitable recombination sites have been rapidly developed. Nevertheless, compared to STAR, alternative tools may be more precise but require parents to be either structurally resolved or phylogenetically well-characterized. Thus, we utilized the STAR method and then performed molecular dynamics (MD) to select crossover sites for recombination of NHase. Furthermore, MD simulation was applied to precisely identify the crossover sites on account of the rigidity of each residue sampled from orbits of stimulation. Both STAR analysis and MD stimulation have successfully predicted the split sites of tryptophan synthase α and TEM-1 β-lactamase, without affecting the normal function of enzymes [25] and change the substrate selectivity of the meta-cleavage product hydrolase [26]. In contrast to

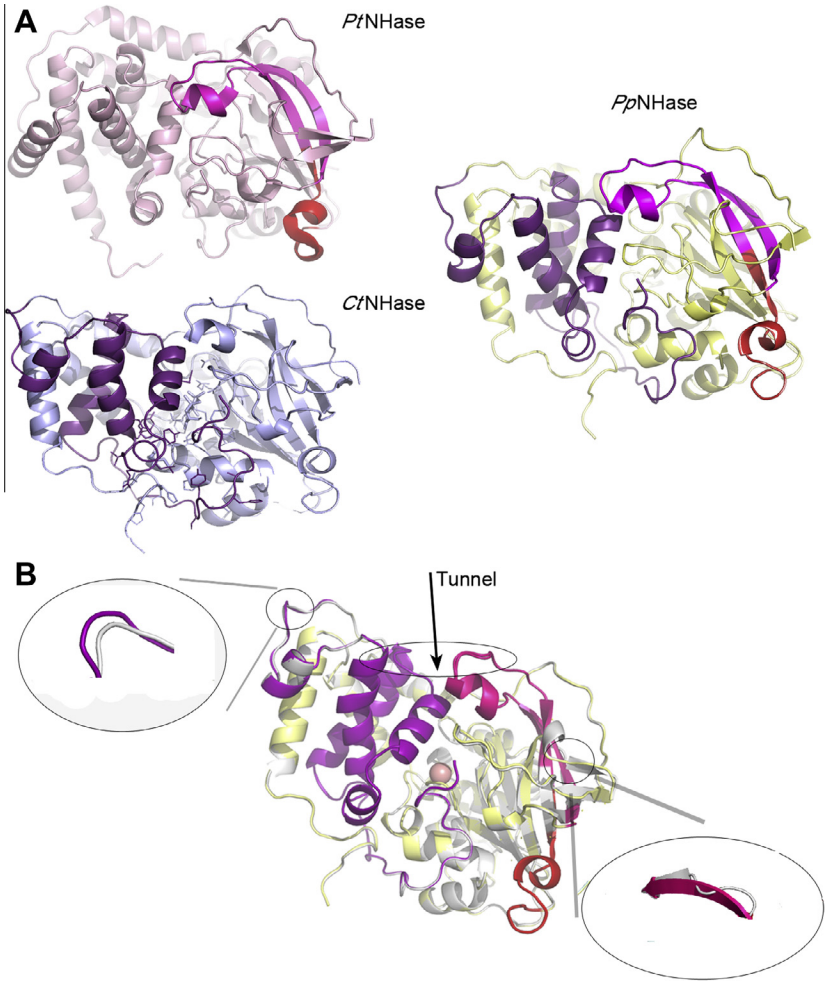


**Fig. 4.** Schematic of the structures of NHases, fragment swapped and tunnels. (A) Three-dimensional structures of *Pp*NHase, *Pt*NHase and *Ct*NHase. (B) The superposition of the 3AB and *Pp*NHase with their tunnels. The structure of *Pp*NHase is in yellow color and that of 3AB in argent color. The selected C-terminal fragments from *Pt*NHase are shown in pink and red; the N-terminal fragment from *Ct*NHase is shown in the magenta. The corresponding fragments in *Pp*NHase are shown in the same colors. The catalytic center is the cobalt colored in light brown. The structural superposition indicates that the 3AB and *Pp*NHase structures are identical except for the flexible β186–191 loop and β250–254 helix for 3AB (sheet for *Pp*NHase), which are indicated by a dotted circle and magnified. The catalytic tunnels are predicted by MOLE 2.0 and labeled by arrows. (For interpretation of the references to color in this figure legend, the reader is referred to the web version of this article.)

these cases, our work expands the methods of improving the stability of the enzyme while maintaining activity.

On the basis of the results from the homology modeling (Fig. 4B) and CD spectrum (Fig. 3C), 3AB resembles the wild-type *Pp*NHase in secondary structure. Thus, instead of the changes in the structures, other factors may be related to the improvement in activity, thermostability and amide-tolerance.

Because all of the swapped fragments do not belong to the active-site residues, it is possible that the attunement of remote residues affect the activity of NHase according to the hypothesis "participation of remote residues in the catalytic activity" [27]. It has been reported that the acrylonitrile (substrate) and acrylamide (product) tunnel can influence NHase activity [28]. Though the location of the tunnel does not change after fragments swapping, two alters between the *Pp*NHase and 3AB are observed according to the results of homology modeling (Fig. 4B). The two alters should result from the two swapped fragments, and then affect the tunnel for substrate and product spreading. As a result, the *K*m of the 3AB decreased by 9 times and *k*cat/*K*m of the 3 AB increased by 7 times. Previous studies have investigated the method to improve the thermostability of NHase, such as introducing salt-bridges [22] and stabilizing the interfacial-subunit [6]. Because the N-terminal domain of *Ct*NHase can interact with α-subunit [29], the fragment may serve to stabilize the interfacial-subunit. Meanwhile, the additional β250–254 helix existing in the C-terminal fragment of 3AB is different from wild-type *Pp*NHase, the salt-bridges among amino acids in 3AB may be changed. Therefore, the fragment swapping method may exploit the advantages of both methods.

## Acknowledgments

This work is financially supported by the National High Technology Research and Development Program of China (863 Program, 2014AA021304), the High Foreign Experts Project (GDW20123200114), the Key project of Chinese Ministry of Education (311023), the Project Funded by the Priority Academic Program Development of Jiangsu Higher Education Institutions the 111 Project (No. 111-2-06), the Collaborative Innovation Center for Advanced Industrial Fermentation, Jiangsu Province, the Public Project for Key Laboratory of Industrial Biotechnology, Ministry of Education, Jiangnan University (KLIB-KF201107, KLIB-KF201203), and the National Natural Science Foundation of China (31300087), Natural Sciences Foundation of Jiangsu (BK20130131, BK20130139).

## Appendix A. Supplementary data

Supplementary data associated with this article can be found, in the online version, at http://dx.doi.org/10.1016/j.bbrc.2014.05.127.

## References


[1] M. Kobayashi, S. Shimizu, Metalloenzyme nitrile hydratase: structure, regulation, and application to biotechnology, Nat. Biotechnol. 16 (1998) 733–736.

[2] Y. Asano, Y. Tani, H. Yamada, A new enzyme" nitrile hydratase" which degrades acetonitrile in combination with amidase, Agric. Biol. Chem. 44 (1980) 2251–2252.

[3] I. Endo, M. Odaka, M. Yohda, An enzyme controlled by light: the molecular mechanism of photoreactivity in nitrile hydratase, Trends Biotechnol. 17 (1999) 244–248.

[4] M. Kobayashi, S. Shimizu, Cobalt proteins, Eur. J. Biochem. 261 (1999) 1–9.

[5] T. Nagasawa, H. Shimizu, H. Yamada, The superiority of the third-generation catalyst: *Rhodococcus rhodochrous* J1 nitrile hydratase, for industrial production of acrylamide, Appl. Microbiol. Biotechnol. 40 (1993) 189–195.

[6] J. Chen, H. Yu, C. Liu, J. Liu, Z. Shen, Improving stability of nitrile hydratase by bridging the salt-bridges in specific thermal-sensitive regions, J. Biotechnol. 164 (2012) 354–362.

[7] T. Davids, M. Schmidt, D. Böttcher, U.T. Bornscheuer, Strategies for the discovery and engineering of enzymes for biocatalysis, Curr. Opin. Chem. Biol. 17 (2013) 215–220.

[8] M.N. Carbone, F.H. Arnold, Engineering by homologous recombination: exploring sequence and function within a conserved fold, Curr. Opin. Struct. Biol. 17 (2007) 454–459.

[9] P.J. Cross, T.M. Allison, R.C. Dobson, G.B. Jameson, E.J. Parker, Engineering allosteric control to an unregulated enzyme by transfer of a regulatory domain, Proc. Natl. Acad. Sci. U.S.A. 110 (2013) 2111–2116.

[10] R.L. Koder, J.L.R. Anderson, L.A. Solomon, K.S. Reddy, C.C. Moser, P.L. Dutton, Design and engineering of an O-2 transport protein, Nature 458 (2009) 305–364.

[11] C.A. Voigt, C. Martinez, Z.G. Wang, S.L. Mayo, F.H. Arnold, Protein building blocks preserved by recombination, Nat. Struct. Biol. 9 (2002) 553–558.

[12] D.C. Bauer, M. Boden, R. Thier, E.M. Gillam, STAR: predicting recombination sites from amino acid sequence, BMC Bioinformatics (2006) 437.

[13] T. Yamaki, T. Oikawa, K. Ito, T. Nakamura, Cloning and sequencing of a nitrile hydratase gene from *Pseudonocardia thermophila* JCM3095, J. Ferment. Bioeng. 83 (1997) 474–477.

[14] M.S. Payne, S. Wu, R.D. Fallon, G. Tudor, B. Stieglitz, I.M. Turner, M.J. Nelson, A stereoselective cobalt-containing nitrile hydratase, Biochemistry 36 (1997) 5447–5454.

[15] M. Laible, K. Boonrod, Homemade site directed mutagenesis of whole plasmids, J. Vis. Exp. (2009) 1135.

[16] Z. Zhou, Y. Hashimoto, K. Shiraki, M. Kobayashi, Discovery of posttranslational maturation by self-subunit swapping, Proc. Natl. Acad. Sci. U.S.A. 105 (2008) 14849–14854.

[17] J.C. Phillips, R. Braun, W. Wang, J. Gumbart, E. Tajkhorshid, E. Villa, C. Chipot, R.D. Skeel, L. Kale, K. Schulten, Scalable molecular dynamics with NAMD, J. Comput. Chem. 26 (2005) 1781–1802.

[18] A.D. MacKerell, D. Bashford, M. Bellott, R.L. Dunbrack, J.D. Evanseck, M.J. Field, S. Fischer, J. Gao, H. Guo, S.A. Ha, et al., All-atom empirical potential for molecular modeling and dynamics studies of proteins, J. Phys. Chem. B 102 (1998) 3586–3616.

[19] Z. Zhou, Y. Hashimoto, K. Shiraki, M. Kobayashi, Discovery of posttranslational maturation by self-subunit swapping, Proc. Natl. Acad. Sci. U.S.A. 105 (2008) 14849–14854.

[20] Y. Liu, W. Cui, Y. Xia, Y. Cui, M. Kobayashi, Z. Zhou, Self-subunit swapping occurs in another gene type of cobalt nitrile hydratase, PLoS One 7 (2012) e50829.

[21] K.L. Petrillo, S. Wu, E.C. Hann, F.B. Cooling, A. Ben-Bassat, J.E. Gavagan, R. DiCosimo, M.S. Payne, Over-expression in *Escherichia coli* of a thermally stable and regio-selective nitrile hydratase from *Comamonas testosteroni* 5-MGAM-4D, Appl. Microbiol. Biotechnol. 67 (2005) 664–670.

[22] J. Liu, H. Yu, Z. Shen, Insights into thermal stability of thermophilic nitrile hydratases by molecular dynamics simulation, J. Mol. Graphics Modell. 27 (2008) 529–535.

[23] K.M. Polizzi, A.S. Bommarius, J.M. Broering, J.F. Chaparro-Riggers, Stability of biocatalysts, Curr. Opin. Chem. Biol. 11 (2007) 220–225.

[24] D. Sehnal, R. Svobodova Varekova, K. Berka, L. Pravda, V. Navratilova, P. Banas, C.-M. Ionescu, M. Otyepka, J. Koca, MOLE 2.0: advanced approach for analysis of biomacromolecular channels, J. Cheminformatics 5 (2013) 39.

[25] Y. Chen, S. Li, T. Chen, H. Hua, Z. Lin, Random dissection to select for protein split sites and its application in protein fragment complementation, Protein Sci. 18 (2009) 399–409.

[26] H. Zhou, Y. Qu, E. Shen, C. Kong, X. Zhang, Q. Ma, J. Zhou, Tuning the substrate selectivity of meta-cleavage product hydrolase by domain swapping, Appl. Microbiol. Biotechnol. 97 (2013) 5343–5350.

[27] H.R. Brodkin, W.R.P. Novak, A.C. Milne, J.A.D. Aquino, N.M. Karabacak, I.G. Goldberg, J.N. Agar, M.S. Payne, G.A. Petsko, M.J. Ondrechen, D. Ringe, Evidence of the participation of remote residues in the catalytic activity of co-type nitrile hydratase from *Pseudomonas putida*, Biochemistry 50 (2011) 4923–4935.

[28] L. Peplowski, K. Kubiak, W. Nowak, Mechanical aspects of nitrile hydratase enzymatic activity. Steered molecular dynamics simulations of *Pseudonocardia thermophila* JCM 3095, Chem. Phys. Lett. 467 (2008) 144–149.

[29] A. Miyanaga, S. Fushinobu, K. Ito, T. Wakagi, Crystal structure of cobalt-containing nitrile hydratase, Biochem. Biophys. Res. Commun. 288 (2001) 1169–1174.